

Supporting Information

Tuning the magnetic properties of metal-oxide nanocrystal heterostructures by cation exchange

Mykhailo Sytnyk,¹ Raimund Kirchschlager,¹ Maryna I. Bodnarchuk,^{2,3} Daniel Primetzhofer,⁴ Dominik Kriegner,¹ Herbert Enser¹., Julian Stangl,¹ Peter Bauer,⁵ Michael Voith,⁶ Achim W. Hassel,⁶ Frank Krumeich,² Frank Ludwig,⁷ Arno Meingast,⁸ Gerald Kothleitner,⁸ Maksym V. Kovalenko,^{2,3} Wolfgang Heiss¹

¹ Institute of Semiconductor and Solid State Physics, Johannes Kepler University Linz, 4040 Linz, Austria

² Institute of Inorganic Chemistry, Department of Chemistry and Applied Biosciences, ETH Zurich, CH-8093, Switzerland

³ Laboratory for Thin Films and Photovoltaics, EMPA-Swiss Federal Laboratories for Materials Science and Technology, CH-8060, Switzerland

⁴ Ion physics, Department of Physics and Astronomy, Uppsala University, 75120 Uppsala, Sweden

⁵ Institute of Experimental Physics, Johannes Kepler University Linz, 4040 Linz, Austria

⁶ Institute for Chemical Technology of Inorganic Materials, Johannes Kepler University, 4040 Linz, Austria

⁷ Institut für Elektrische Messtechnik und Grundlagen der Elektrotechnik, TU Braunschweig, 38106 Braunschweig, Germany

⁸ Austrian Centre for Electron Microscopy and Nanoanalysis, Institute for Electron Microscopy, Graz University of Technology, 8010 Graz, Austria

Experimental Methods

Synthesis of the ferrite based magnetic nanocrystals

Iron oxide nanocrystals

The Fe_3O_4 NCs were synthesized by thermal decomposition of iron oleate at 315°C .¹ Iron oleate was prepared from FeCl_3 , NaOH and oleic acid in methanol. For the synthesis, 2.3 mmol of iron oleate, 1.15 mmol of oleic acid and 15 mL of octadecene were loaded into a flask and dried under vacuum for 30 min at 120°C . After that the reaction mixture was heated to the refluxing temperature of the mixture (315°C) with heating rate of $3.3^\circ\text{C}/\text{min}$. The growth time of the Fe_3O_4 NCs was 20 min at 315°C . After cooling to room temperature, the NCs were isolated by adding a hexane/ethanol mixture. The washing step was repeated two times. Finally the NCs were stored in hexane.

Gold/iron oxide core/shell nanocrystals

The Au NCs, acting as cores, were synthesized according to Ref.² Dodecanethiol was used as capping ligand during preparation and as digestive ripening agent in order to narrow the size distribution of the Au NCs. After ripening, the Au NCs were precipitate with ethanol, centrifugated and redispersed in toluene. For the growth of the shell, approximately 7 mg of the Au NCs and 0.1 mL of oleic acid were added to 20 mL octadecene in a flask. The solution was kept at 80°C under vacuum for 30 min. After heating to 180°C , 0.1 mL of $\text{Fe}(\text{CO})_5$ was injected into the solution. The growth time of the Au/ Fe_3O_4 NCs was 30 min. After the growth, air was passed through the solution for 6 min at 180°C and further during cooling down of the solution to room temperature. The Au/ Fe_3O_4 NCs were washed with a toluene/ethanol mixture.³

Wüstite/metal ferrite nanocrystals

The $\text{Fe}_x\text{O}/\text{CoFe}_2\text{O}_4$ nanocrystals were synthesized by thermal decomposition of iron- and cobalt-oleates at 318°C .⁴ A $\text{Fe}^{(3+)}\text{Co}^{(2+)}$ -oleate mixture was prepared from FeCl_3 and CoCl_2 in the presence of sodium oleate and oleic acid in methanol. In the synthesis of $\text{Fe}_x\text{O}/\text{CoFe}_2\text{O}_4$ nanocrystals, a solution of $\text{Fe}^{(3+)}\text{Co}^{(2+)}$ -oleates in octadecene with concentration of 0.2mol/kg was used. 15 mL of this solution was mixed with 0.42 mL oleic acid (oleate:oleic acid molar ratio ~2:1) and dried under vacuum for 60 min at 110°C . Then the reaction mixture was heated up under Argon to 318°C at a constant rate of $2^\circ\text{C}/\text{min}$. Afterwards, the solution was kept at this temperature for 10 min and cooled down to room temperature. The nanocrystals were isolated

by adding a chloroform/acetone mixture. The washing step was repeated 2 times. Finally, nanocrystals were redispersed in solvents such as chloroform, hexane, and toluene.

Structural characterization

TEM analysis

High-resolution TEM microscopy was carried out using a JEOL 2200FS microscope operated at 200 kV with a point resolution of 0.23nm. The scanning transmission electron microscopy (STEM) investigations were performed on the aberration-corrected HD-2700CS (Hitachi; cold-field emitter), operated at an acceleration potential of 200 kV. A probe corrector (CEOS) is incorporated in the microscope column between the condenser lens and the probe-forming objective lens providing excellent high-resolution capability (the beam diameter is approximately 0.1 nm in the ultra-high resolution mode). Different detectors have been chosen for imaging in bright field (BF) and dark field mode ((high-angle) annular dark field ((HA)ADF)). The variation of the collection angles in bright field mode allows one to record images either with a high contribution of the direct beam (so-called wide angle mode (WAM); mainly mass-thickness contrast) or with diffracted beams included in such a way that an almost pure phase contrast is obtained (phase contrast mode (PCM); interference pattern). Furthermore, a secondary electron (SE) detector is used inside the column of the HD-2700CS microscope above the sample allowing the study of the sample morphology as well. The images (1024 x 1024 pixels) were recorded with frame times of 20 s.

Rutherford backscattering spectrometry

Rutherford Backscattering spectrometry was performed employing the 5 MeV Tandem accelerator at Uppsala University. 8 MeV $^{12}\text{C}^{3+}$ ions were used as primary particles. This specific energy-projectile combination was chosen since it permits an excellent separation of the signals obtained from Fe and Co while featuring sufficiently high scattering cross sections in order to get good statistics. A solid state detector situated in a backscattering angle Θ of 170° was used to detect scattered projectile ions. Beam currents were kept around 1 – 3 nA to ensure a destruction free analysis. In consequence no alteration of spectra due to ion beam induced damage was observed during the runs. The experimental data were analyzed using the SIMNRA simulation package.⁵ By fitting the two distinct peaks obtained from backscattering from Fe and

Co using appropriate potentials it is straightforward possible to obtain the respective concentrations.

X ray diffraction

Synchrotron x-ray powder diffraction measurements were performed at the high resolution powder diffraction beamline P02.1 at Petra III/HASYLAB Hamburg. The measurements were performed using 60keV synchrotron radiation. Data collection was done with a Perkin Elmer XRD1621 two dimensional detector at a distance of 541mm. For the measurements, performed in transmission geometry, the nanocrystals were transferred onto an adhesive tape. The 2 dimensional detector images show X-ray diffraction powder rings. For data analysis, however, line scans from these were used, as obtained by angular integration. The obtained line scans are plotted versus the momentum transfer Q defined as $4\pi/\lambda \sin(2\Theta/2)$ with the angle 2Θ measured between the scattered and primary beam. The lattice parameters were quantified using the Rietveld method via the MAUD software package.⁶ The cubic Wüstite-like phase of FeCoO was used as a core and the cubic Spinel structure of CoFe_2O_4 as shell. Core and shell were assumed to be independent for the fitting.

Atomic absorption spectroscopy

All reagents used for the composition analysis performed by atomic absorption spectrometry were of analytical grade. The nanocrystal samples were dissolved in sulfuric acid (Merck, Germany) and diluted with deionized water in a 100 ml volumetric flask. Standard solutions for analysis were produced by diluting stock solutions of iron (1000 mg/l) and cobalt (1000 mg/l) salts in deionized water containing sulfuric acid with deionized water. Also a blank solution was used during experiments, prepared by diluting proper amounts of sulfuric acid with deionized water. The experiments were performed in a HITACHI Z-8230 Polarized Zeeman Atomic Absorption Spectrophotometer with background correction, equipped with digital data acquisition and processing. The atomization of the solutions was realized by an Air-Acetylene flame (15.0 l/min air, 2.1 l/min acetylene), and the wavelengths were 248.3 nm for iron and 240.7 nm for cobalt. The calibration was carried out by measuring blank and standard solutions and the obtained calibration curves were fitted by linear regression.

Magnetic characterization

SQUID magnetometry

The magnetic properties were measured using a Quantum Design MPMS-2 SQUID magnetometer. The samples were prepared by placing 0.5 to 2 mg of powdered nanocrystals into gelatin capsules. The exact weight of the total amount of Co and Fe present in the samples was determined by AAS. For that purpose the samples were dissolved completely in sulfuric acid. The AAS ensures that the weight of ligand molecules or other organic residuals, which are present in the NC solutions, do not affect the weight determination of the magnetic materials. The zero field cooled magnetization experiments were measured under an applied field of 100 Oe. To measure the exchange bias effect, the samples were cooled down from 350 K under an applied field of 1 T. The hysteresis loops were performed after reversing the field direction two times and after applying waiting times up to 20 min before the measurements were started. At each temperature the field reversal and waiting steps were repeated.

Fluxgate magnetorelaxometry

A home built fluxgate magnetorelaxometer was used to measure the magnetic moments of the nanocrystals after aligning them by a magnetization pulse of 2 s lengths and 2 mT magnitude. After abruptly switching off the magnetization field, the decay of the net magnetic moment of the samples is measured utilizing a differential fluxgate sensor setup.⁷ The nanocrystals were immobilized on a substrate so that the relaxation signal reflects the internal Néel relaxation with a relaxation time constant which is given by $\tau_N = \tau_0 \exp\left[\frac{KV}{k_B T}\right]$. The time τ_0 is generally assumed to be about 10^{-9} s, K is the anisotropy constant, V the NC volume, and $k_B T$ the thermal energy. Thus, different Néel time constants directly reflect different anisotropy energies.

- [1] M. V. Kovalenko, M. I. Bodnarhchuk, R. T. Lechner, G. Hesser, F. Schäffler, W. Heiss, *J. Am. Chem. Soc.* **2007**, *129*, 6352-6353
- [2] B. L. V. Prasad, S. I. Stoeva, C. M. Sorensen, K. J. Klabunde, *Langmuir* **2002**, *18*, 7515-12
- [3] E. V. Shevchenko, M. I. Bodnarchuk, M. V. Kovalenko, D. V. Talapin, R. K. Smith, S. Aloni, W. Heiss, A. P. Alivisatos. *Adv. Mater.*, **2008**, *20*, 4323-4329
- [4] M. I. Bodnarchuk, M. V. Kovalenko, H. Groiss, R. Resel, M. I. Reissner, G. Hesser, R. T. Lechner, W. Steiner, F. Schäffler, W. Heiss. *Small*, **2009**, *5*, 2247-2252
- [5] M. Mayer, *Application of Accelerators in Research and Industry*. **1999**, *475*, 541
- [6] L. Lutterotti, S. Matthies, H. R. Wenk; *IUCr: Newsletter of the CPD* **1999**, *21*, 14-15
- [7] F. Ludwig, S. Mäuselein, E. Heim, M. Schilling, *Rev. Sci. Instrum.* **2005**, *76*, 106102

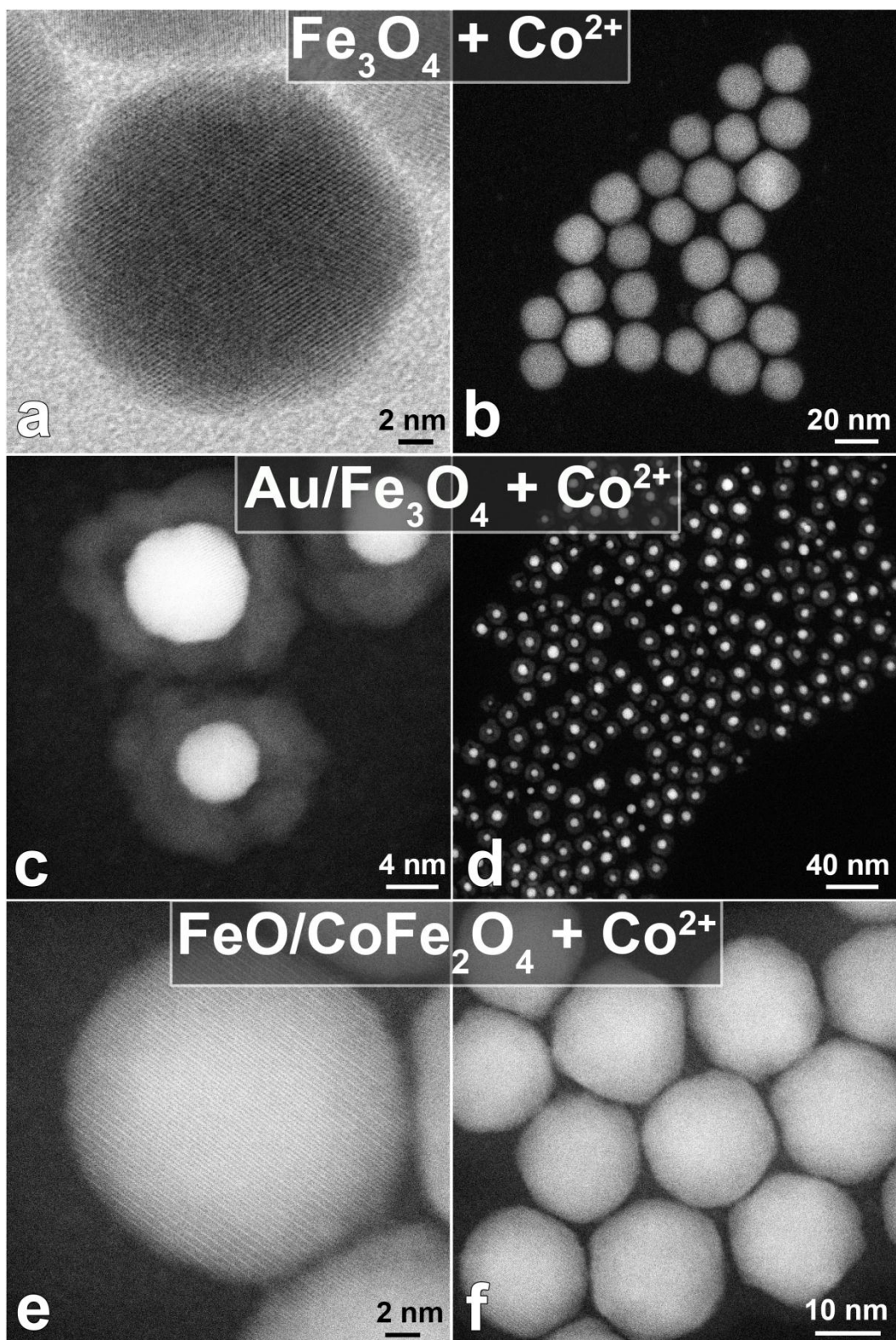


Figure S1 Wide angle mode bright field STEM image, (a), and high angle dark field STEM (Z-contrast) images, (b-f), of the nanocrystals, after the Fe^{2+} to Co^{2+} cation exchange treatment was performed. (a,b) Homogeneous nanocrystals, (b-c) gold/ Fe_2O_3 core shell nanocrystals, (e-f) $\text{FeO}/\text{CoFe}_2\text{O}_4$ core/shell nanocrystals.

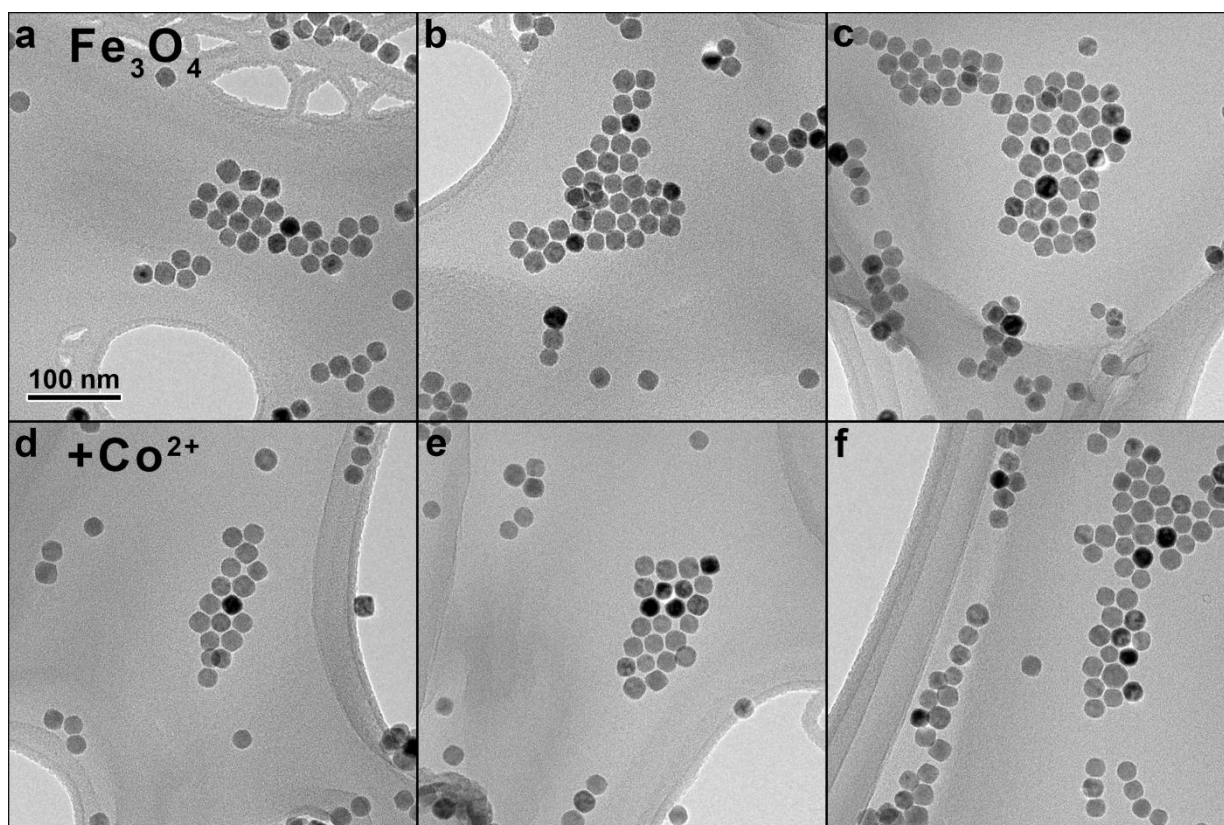


Figure S2 TEM images used to extract the size distributions shown in Figure 2(b) and (c). Approximately 200 nanocrystals are used for the size distributions before, (a-c), and after the Co^{2+} treatment (d-f).

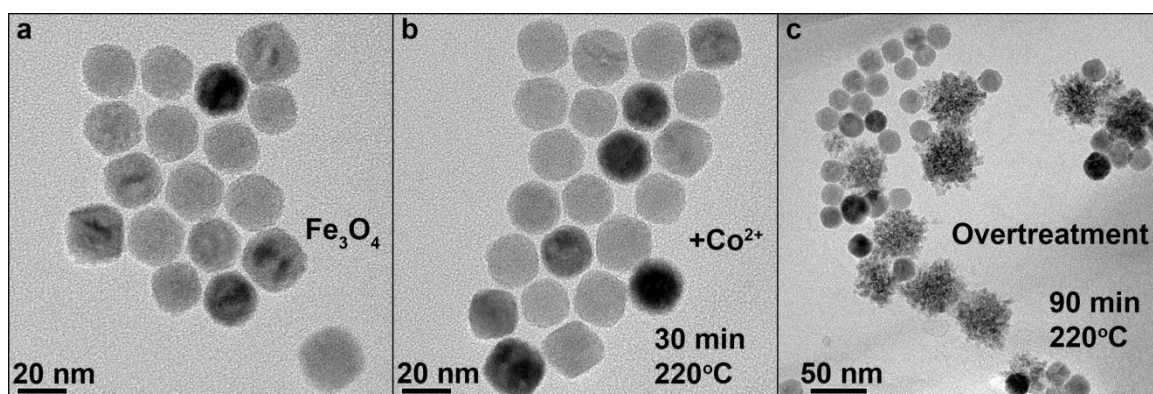


Figure S3 Effect of Co^{2+} treatment on Fe_3O_4 nanocrystals with a mean size of 21 nm. (a) TEM images of the initial nanocrystals, (b), of the nanocrystals after a treatment time of 30 min, (c), and after 90 min. While after 30 min homogeneous spherical nanocrystals with a Co concentration of 8% are obtained, a too long treatment time (overtreatment) results in dissolution of a part of the nanocrystals and the formation of irregular aggregates of much smaller nanoparticles.

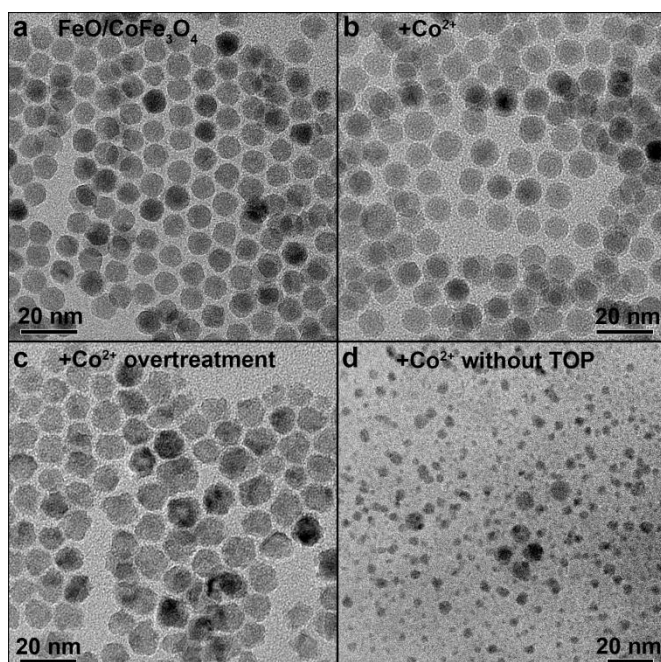


Figure S4 Effect of Co^{2+} treatment on $\text{FeO}/\text{CoFe}_3\text{O}_4$ core/shell nanocrystals with a mean size of 8 nm. (a,b) After a treatment time of 40 min performed at a temperature of 200 °C the size and size distribution is almost preserved, (c) whereas too long treatment times result in a severe change of nanocrystal size. (d) If the Co treatment is performed at the same temperature but without the addition of TOP, the nanocrystals are dissolved and only very small nanoparticles can be found by TEM imaging.

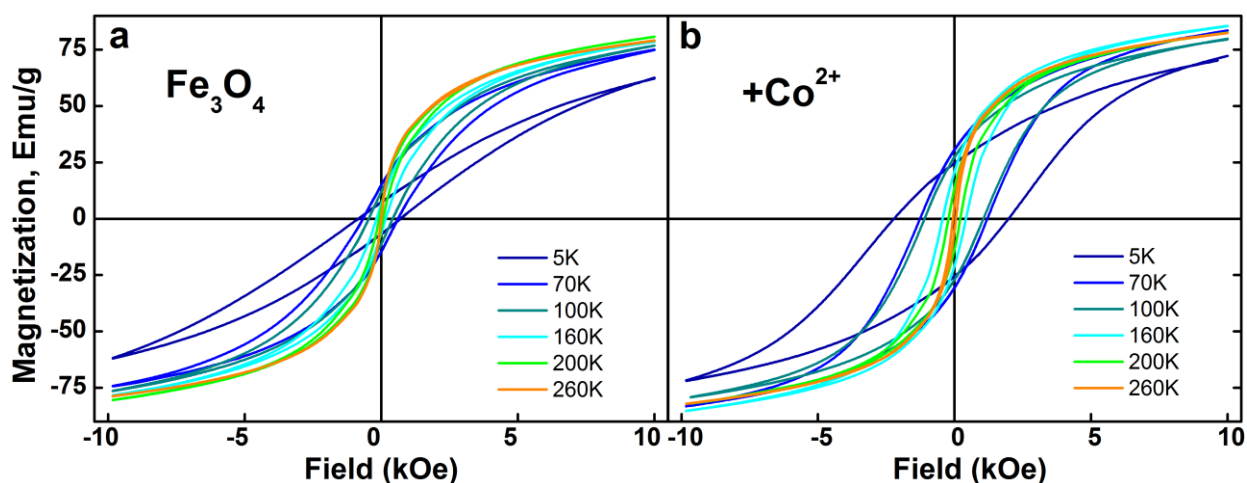


Figure S5 (a) Hysteresis loops of Fe_3O_4 nanocrystals with a size of 21 nm. (b) After Co^{2+} treatment, resulting in a Co concentration of 8 %, the opening of the hysteresis loops is increased at all temperatures.

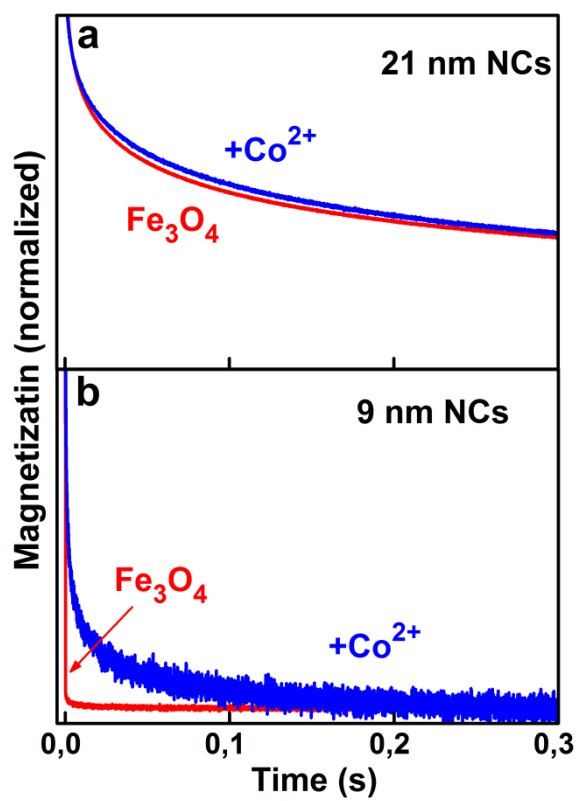


Figure S6 Magnetization relaxation of immobilized Fe₃O₄ nanocrystals before and after Co²⁺ treatment, measured by flux gate magnetometry, (a) for nanocrystals with a mean diameter of 21 nm, and (b) of 9 nm.

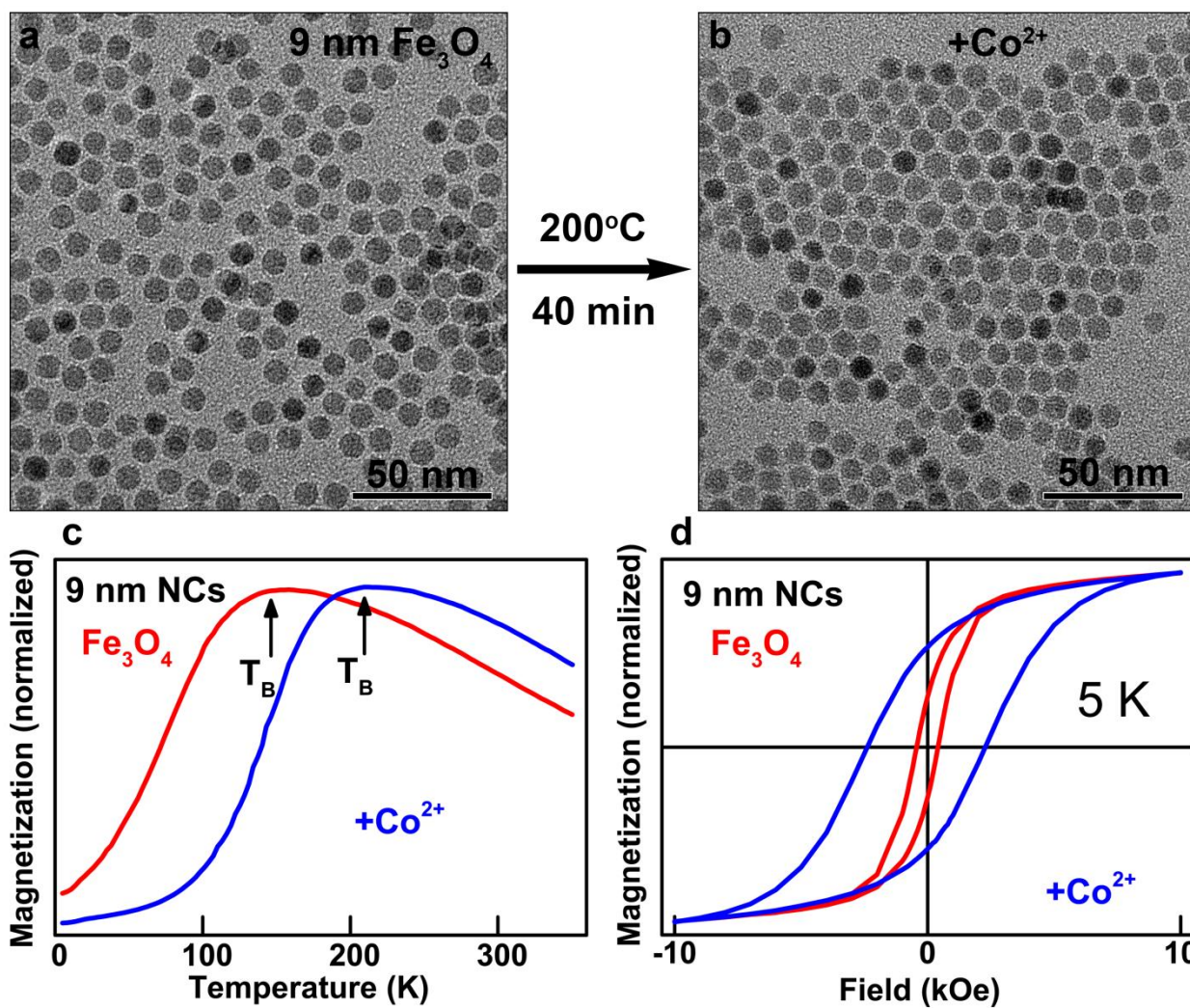


Figure S7 Results for small Fe_3O_4 nanocrystals with a mean diameter of 9 nm. (a, b) The Co^{2+} treatment performed at 200 °C for 40 min preserves the size and size distribution. (c) The blocking temperature T_B increases from 130 K to 210 K. (d) The opening of the hysteresis loop observed a 5 K increase from 836.6 Oe to 4 674.8 Oe.

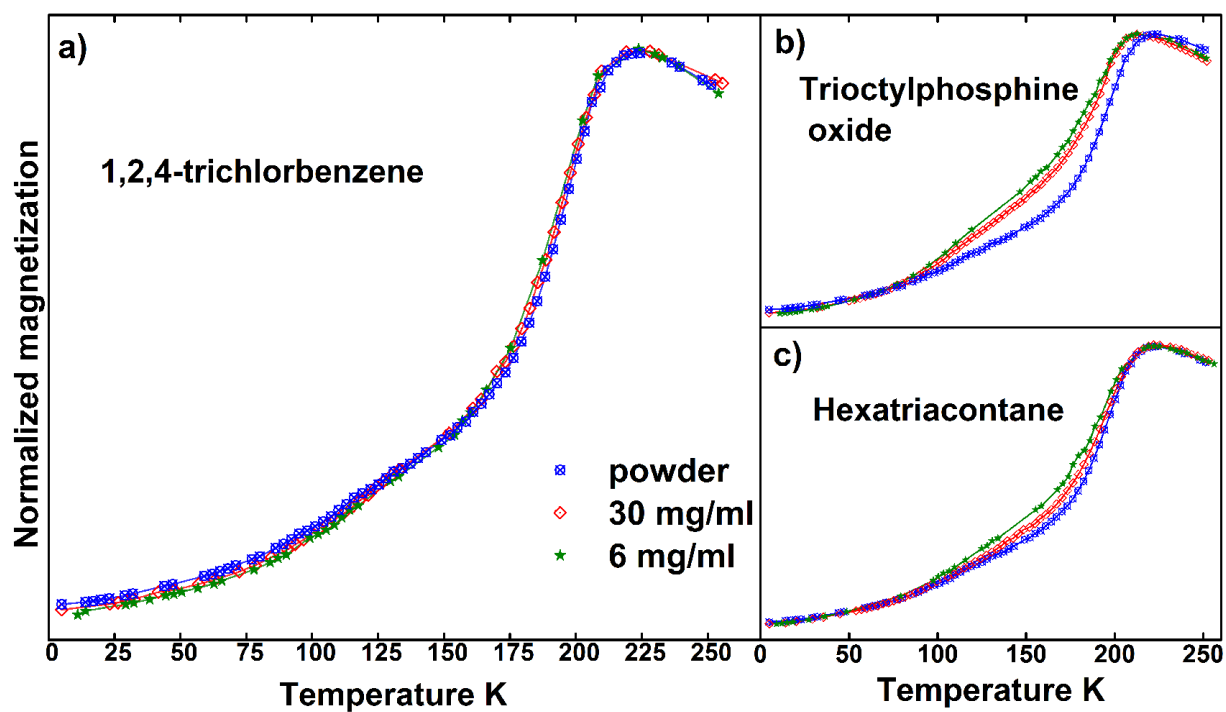


Figure S8 Solvent dependent magnetization of Fe_3O_4 nanocrystals with a mean size of 14 nm. (a) In trichlorobenzene the nanocrystals give a stable colloidal solution and the magnetization curves exhibit the same shape as the powder sample, independent of dilution. (b) Diluting in TOP gives a stable colloidal solution and causes a small decrease of the blocking temperature, because the nanocrystals surface is reacting with TOP. (c) Solving in hexatriacontane causes visible aggregates in solution, which does not have an effect on the superparamagnetic blocking temperature, but changes the shape of the magnetization curve.

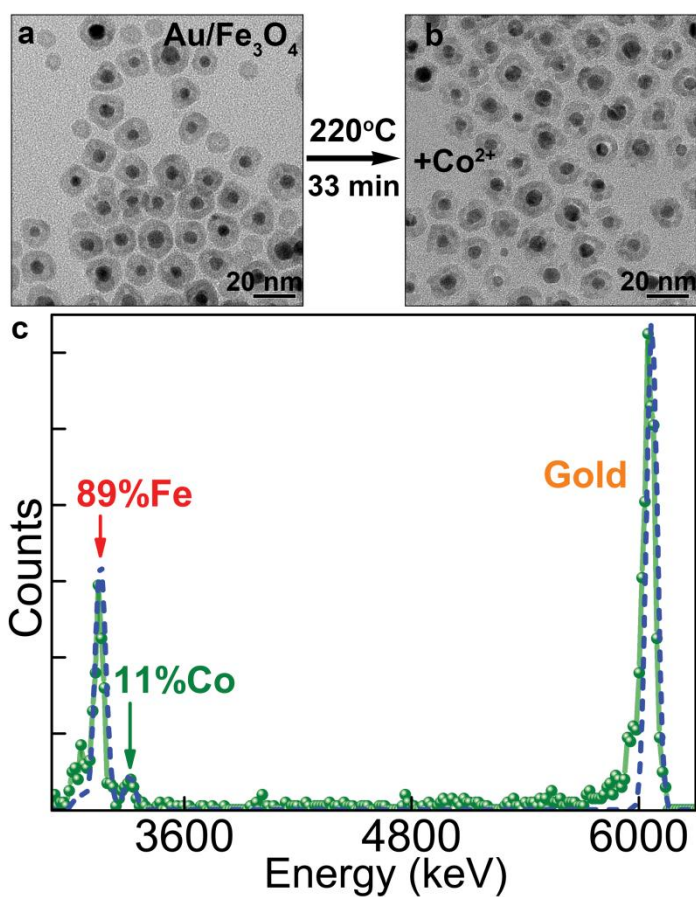
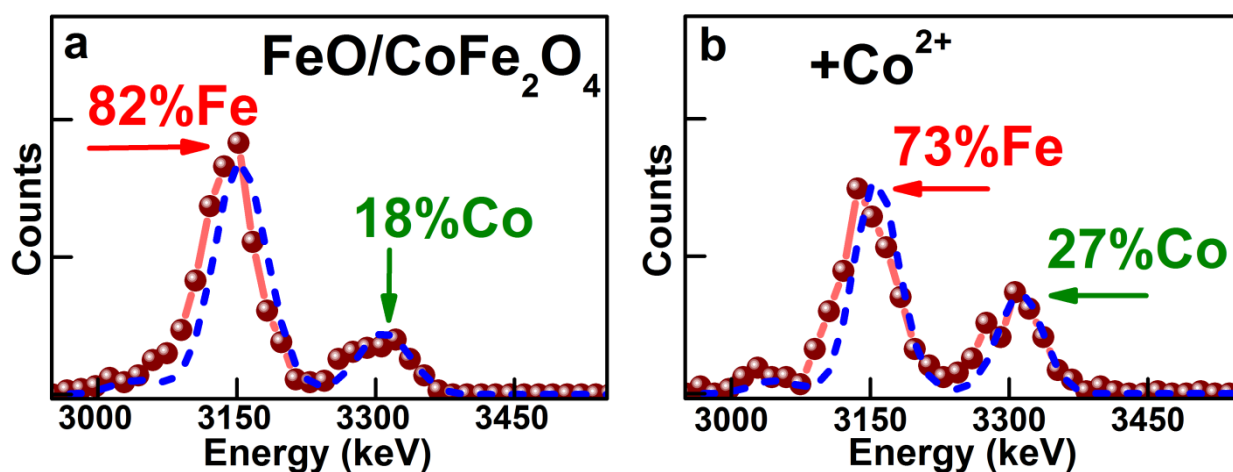
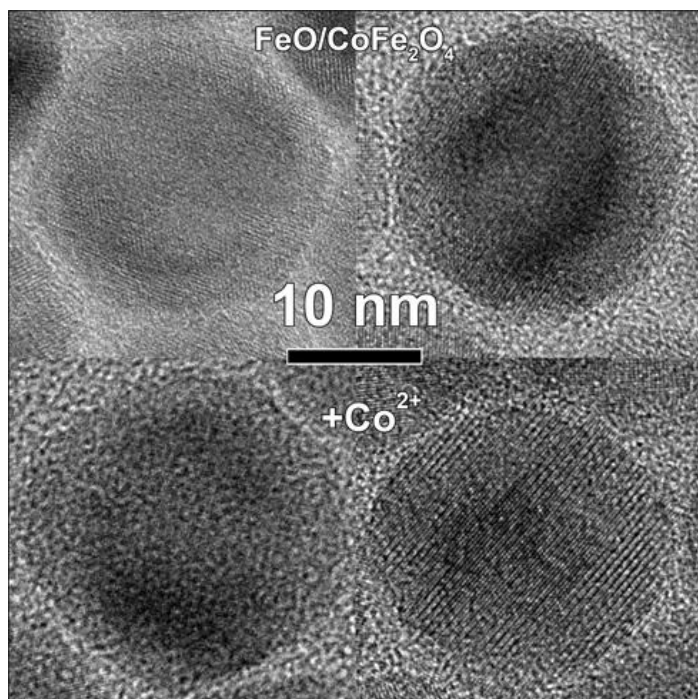


Figure S9 Au/Fe₃O₄ core/shell nanocrystals before, (a), and after, (b), Co²⁺ treatment. (c) The Co²⁺ concentration of 11 % is determined by fitting Rutherford backscattering spectrometry data.



Figures S10 Rutherford backscattering data of the FeO/CoFe₂O₄ core/shell nanocrystals with a size of 21 nm, shown in Figures 4 -6.



Figures S11 TEM images of the FeO/CoFe₂O₄ nanocrystals before (top panels) and after (bottom panels) cation exchange. The shrinking of the core and growth of shell, which can be seen here by comparing the two images on the right side, is evidenced by X-ray diffraction experiments, performed on a nanocrystal assemble.